Electronic Supplementary Material (ESI) for Green Chemistry

Supplementary Information for

One-pot selective conversion of furfural into 1,5-pentanediol over Pd -added Ir-ReO_x/SiO_2 bifunctional catalyst

Sibao Liu, Yasushi Amada, Masazumi Tamura, Yoshinao Nakagawa* and Keiichi Tomishige*

Department of Applied Chemistry, School of Engineering, Tohoku University,

6-6-07, Aoba, Aramaki, Aoba-ku, Sendai 980-8579, Japan

*Corresponding authors: Keiichi Tomishige and Yoshinao Nakagawa

School of Engineering, Tohoku University,

6-6-07, Aoba, Aramaki, Aoba-ku, Sendai, 980-8579, Japan

E-mail: tomi@erec.che.tohoku.ac.jp

yoshinao@erec.che.tohoku.ac.jp

Table S1. Conversion of furfural over Pd(0.66)-Ir-ReO_x/SiO_2 at different furfural concentration

Entry	Concentration / %	Conversion / %	Yield / %								
			1,5-PeD	1,4-PeD	1,2-PeD	1-PeOH	2-PeOH	THFA	FFA	2-MTHF	Others
1	5	>99.9	61.2	5.5	1.3	10.3	0.7	10.3	0.0	3.4	7.4
2	10	>99.9	63.2	5.3	1.3	12.5	0.6	10.2	0.0	3.0	3.9
3	20	>99.9	59.5	6.3	1.4	16.6	1.0	4.9	0.0	4.7	5.5
4	50	>99.9	34.1	3.5	1.5	10.4	0.4	31.7	0.0	3.3	15.1

PeD: pentanediol; PeOH: pentanol; THFA: tetrahydrofurfuryl alcohol; FFA: furfuryl alcohol; 2-MTHF: 2-methyltetrahydrofuran.

Pretreatment: 473 K, H_2 (8 MPa), 1 h.

Reaction conditions: Furfural (1 g), H_2O (1-19 g), Pd(0.66)-Ir-ReO_x/SiO_2 (100 mg), initial H_2 (6 MPa), T_1: 313 K, time 1: 2 h, T_2: 393 K, time 2: 24 h, 500 rpm.

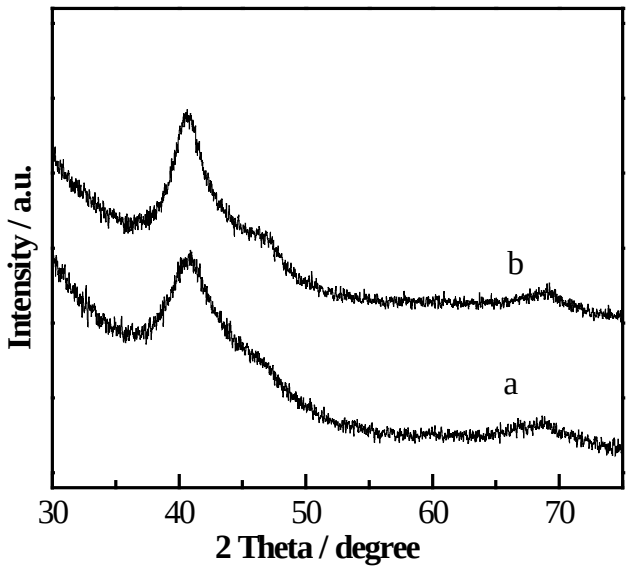

Fig. S1. XRD patterns of Pd(0.66)–Ir–ReO_x/SiO_2 after reduction at 473 K for 1 h (a) and after the fourth use (b).

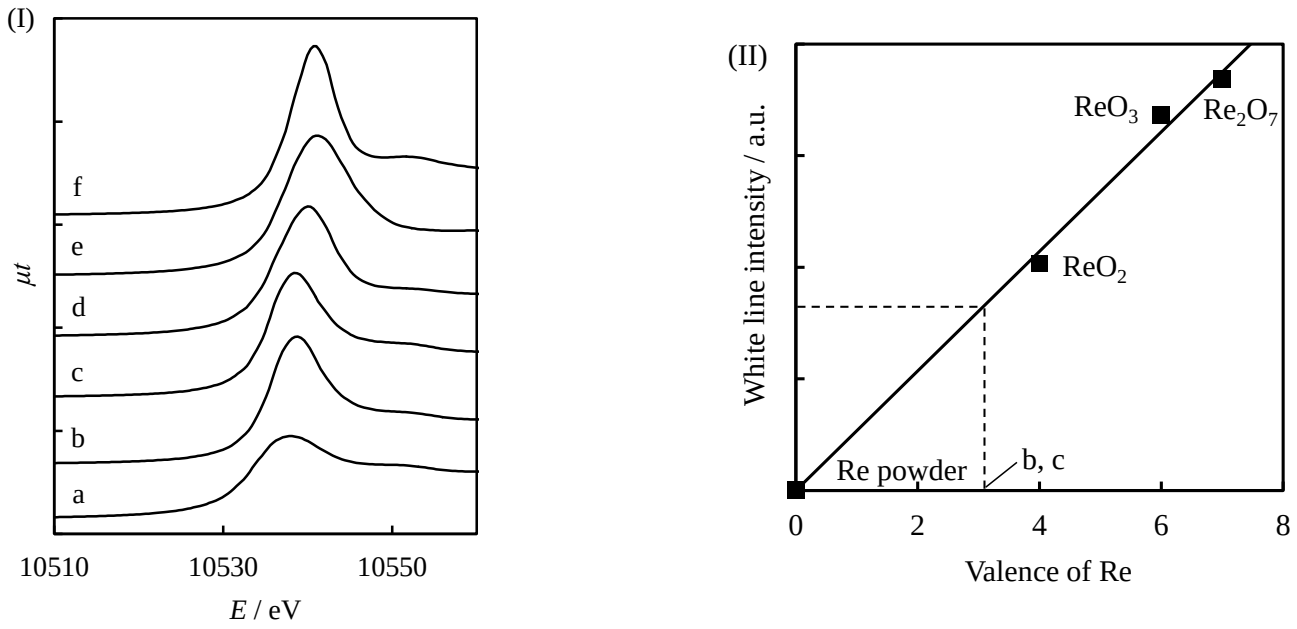

Fig. S2. Results of Re L_3-edge XANES analysis of Ir-ReO_x/SiO_2 and Pd(1.8)–Ir–ReO_x/SiO_2.

(I) Re L_3-edge XANES spectra, (II) Relation between white line area and valence of Re. (a) Re powder, (b) Ir−ReO_x/SiO_2 after the catalytic use, (c) Pd(1.8)−Ir−ReO_x/SiO_2 after the catalytic use and (d) ReO_2, (e) ReO_3 and (f) Re_2O_7.

The method of XANES analysis

The first peak in the L_3-edge XANES is called as a white line, and the white line area in the L_3-edge XANES is known to be an informative indication of the electronic state. The larger white line intensity is due to greater electron vacancy in *d*-orbital. As reported previously, a relative electron deficiency and ionic valence can be determined on the basis of the white line intensity.[S1-S4] Regarding the reference compounds, ionic valence of Re species had almost linear relation to the white line intensity. Therefore, the average value of Re species can be estimated by the examining the white line area in the XANES spectra.[S5, S6]

Table S2. Summary of characterization results of the catalysts

Catalyst	Metal amount / mmol·g_{cat}^{-1}			Valence of Re from XANES	TPR		CO adsorption / mmol·g_{cat}^{-1}
	Pd	Ir	Re		H_2 consumption / mmol·g_{cat}^{-1}	Valence of Re[a]	
Ir-ReO_x/SiO_2	–	0.208	0.416	3.1	0.927	4.5	0.037
Pd-ReO_x/SiO_2	0.062	–	0.416	–	0.845	2.9	–
Pd(0.09)-Ir-ReO_x/SiO_2	0.008	0.208	0.416	–	1.28	2.8	–
Pd(0.22)-Ir-ReO_x/SiO_2	0.021	0.208	0.416	–	1.10	3.7	–
Pd(0.44)-Ir-ReO_x/SiO_2	0.041	0.208	0.416	–	1.12	3.6	–
Pd(0.66)-Ir-ReO_x/SiO_2	0.062	0.208	0.416	–	0.892	4.7	0.058
Pd(0.89)-Ir-ReO_x/SiO_2	0.084	0.208	0.416	–	0.927	4.5	–
Pd(1.8)-Ir-ReO_x/SiO_2	0.166	0.208	0.416	3.1	0.788	5.2	–
Pd(0.66)/SiO_2	0.062	–	–	–	–	–	0.009

[a] 7-2×[(amount of H_2 consumed, mol)-2×(Ir loading amount, mol)]/(Re loading amount, mol).

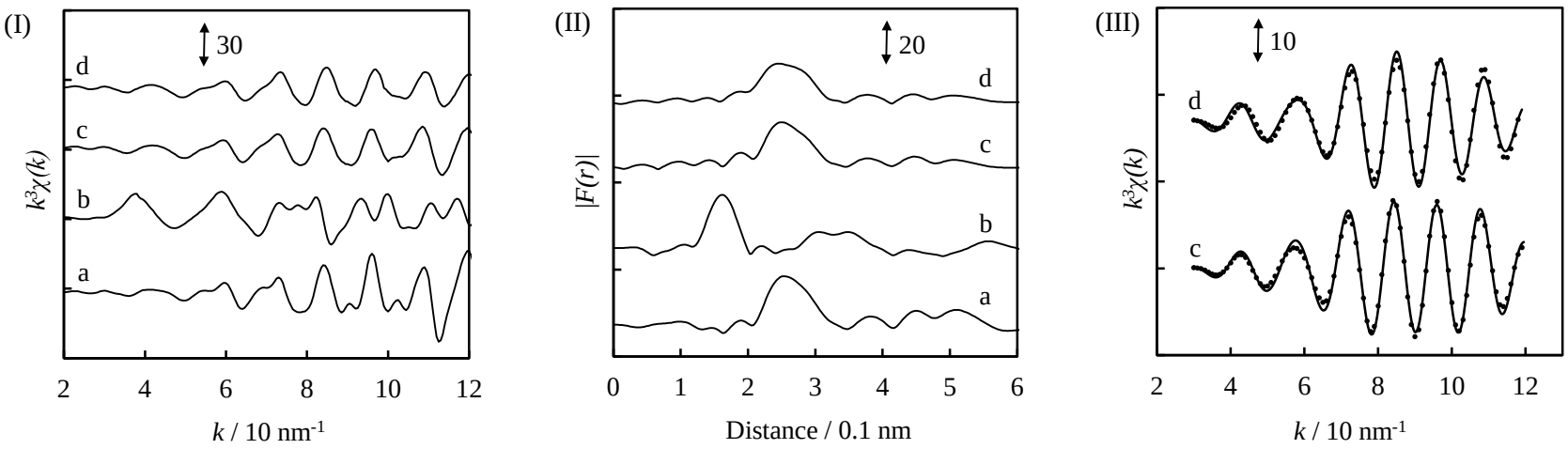

Fig. S3. Results of Ir L_3-edge EXAFS analysis of Ir−ReO_x/SiO_2 and Pd(1.8)−Ir−ReO_x/SiO_2 after the catalytic use.
(I) k^3-Weighted EXAFS oscillations. (II) Fourier transform of k^3-weighted Ir L_3-edge EXAFS, FT range: 30–120nm^{-1}. (III) Fourier filtered EXAFS data (solid line) and calculated data (dotted line), Fourier filtering range: 0.163–0.325 nm. (a) Ir powder, (b) IrO_2, (c) Ir−ReO_x/SiO_2 after hydrogenolysis of glycerol[S7] and (d) Pd(1.8)−Ir−ReO_x/SiO_2 after reduction.

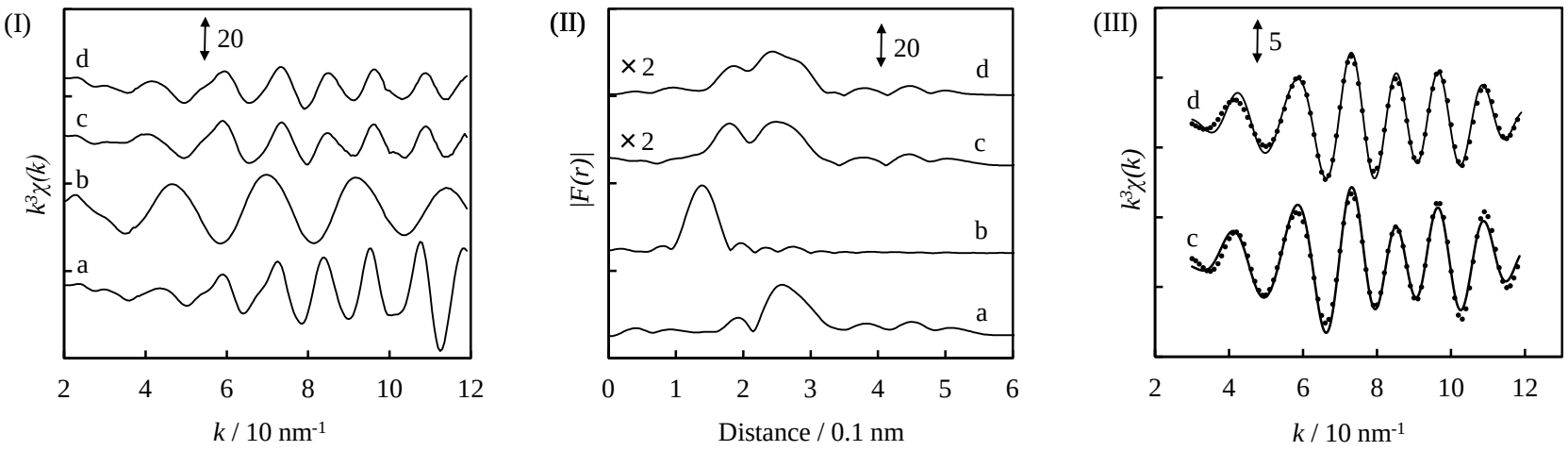

Fig. S4. Results of Re L_3-edge EXAFS analysis of Ir−ReO_x/SiO_2 and Pd(1.8)−Ir−ReO_x/SiO_2 after the catalytic use.
(I) k^3-Weighted EXAFS oscillations. (II) Fourier transform of k^3-weighted Re L_3-edge EXAFS, FT range: 30–120 nm^{-1}. (III) Fourier filtered EXAFS data (solid line) and calculated data (dotted line), Fourier filtering range: 0.138–0.325 nm. (a) Re powder, (b) NH_4ReO_4, (c) Ir−ReO_x/SiO_2 after hydrogenolysis of glycerol [S7] and (d) Pd(1.8)−Ir−ReO_x/SiO_2 after reduction.

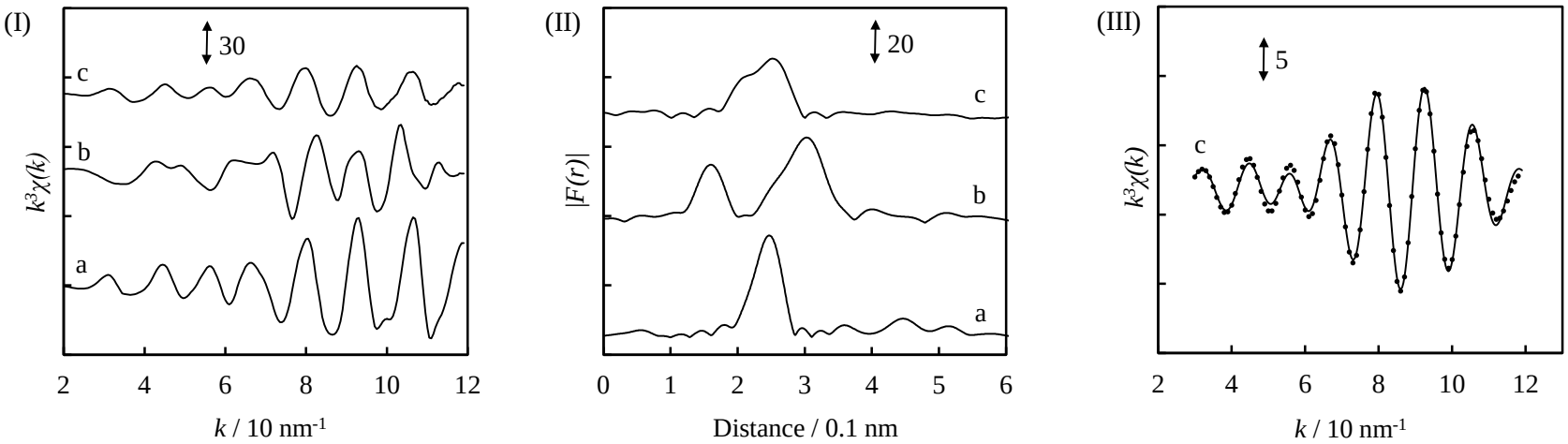

Fig. S5. Results of Pd *K*-edge EXAFS analysis of Pd(1.8)−Ir−ReO_x/SiO_2 after the catalytic use.

(I) k^3-Weighted EXAFS oscillations. (II) Fourier transform of k^3-weighted Pd *K*-edge EXAFS, FT range: 30–120 nm^{-1}. (III) Fourier filtered EXAFS data (solid line) and calculated data (dotted line), Fourier filtering range: 0.135–0.331 nm. (a) Pd foil, (b) PdO, (c) Pd(1.8)−Ir−ReO_x/SiO_2 after reduction.

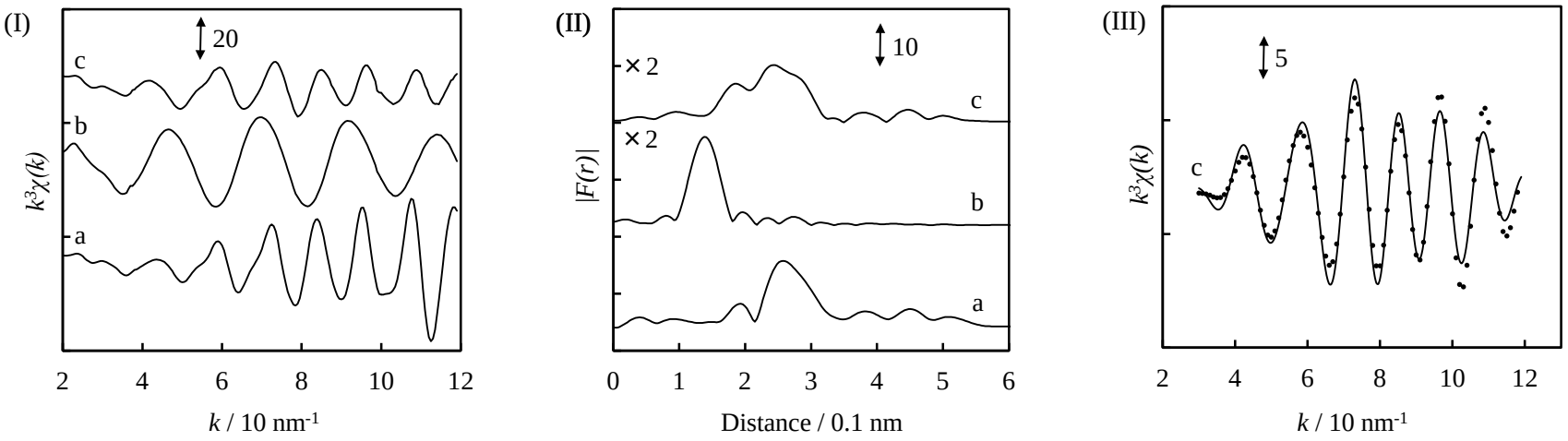

Fig. S6. Results of Re L_3-edge EXAFS analysis of Pd(1.8)−Ir−ReO_x/SiO_2 after the catalytic use without Re-Pd shell.
(I) k^3-Weighted EXAFS oscillations. (II) Fourier transform of k^3-weighted Re L_3-edge EXAFS, FT range: 30–120 nm^{-1}. (III) Fourier filtered EXAFS data (solid line) and calculated data (dotted line), Fourier filtering range: 0.138–0.325 nm. (a) Re powder, (b) NH_4ReO_4 and (c) Pd(1.8)−Ir−ReO_x/SiO_2 after the reduction.

Table S3. Curve fitting results of Re L_3-edge EXAFS of Pd (1.77)-Ir-ReO_x/SiO_2 without Re-Pd shell

Catalyst	Shells	CN[a]	R / 10^{-1} nm[b]	σ / 10^{-1} nm[c]	ΔE_0 / eV[d]	R_f / %[e]
Pd(1.8)-Ir-ReO_x/SiO_2	Re-O	1.7	2.05	0.086	2.1	4.4
	Re-Ir (or -Re)	6.0	2.69	0.080	10.4	
NH_4ReO_4	Re=O	4	1.73	0.06	0	–

[a]Coordination number. [b]Bond distance. [c]Debye-Waller factor. [d]Difference in the origin of photoelectron energy between the reference and the sample. [e]Residual factor. Fourier filtering range: 0.138-0.325 nm.

Reference

S1 T. Kubota, K. Asakura, N. Ichikuni and Y. Iwasawa, *Chem. Phys. Lett.*, 1996, **256**, 445-448.

S2 T. Kubota, K. Asakura and Y. Iwasawa, *Catal. Lett.*, 1997, **46**, 141-144.

S3 A.N. Mansour, J.W. Cook Jr. and D.E. Sayers, *J. Phys. Chem.*, 1984, **88**, 2330-2334.

S4 J.A. Horsely, *J. Chem. Phys.*, 1982, **76**, 1451–1458.

S5 M. Rønning, T. Gjervan, R. Prestivik, D.G. Nicholson and A. Holmen, *J. Catal.*, 2001, **204**, 292–304.

S6 Y. Ishida, T. Ebashi, S. Ito, T. Kubota, K. Kunimori and K. Tomishige, *Chem. Commn.*, 2009, 5308–5310.

S7 Y. Amada, Y. Shinmi, S. Koso, T. Kubota, Y. Nakagawa and K. Tomishige, *Appl. Catal. B: Environ.*, 2011, **105**, 117-127.